Available online at www.sciencedirect.com

jmr&t
Journal of Materials Research and Technology
www.jmrt.com.br

Original Article

Identification of optimum friction stir spot welding process parameters controlling the properties of low carbon automotive steel joints

*A.K. Lakshminarayanan**, V.E. Annamalai, K. Elangovan*

Department of Mechanical Engineering, SSN College of Engineering, Kalavakkam, Tamil Nadu, India

ARTICLE INFO

Article history:
Received 19 September 2014
Accepted 7 January 2015
Available online 7 February 2015

Keywords:
Automotive steel
Friction stir spot welding
Microstructure
Tensile shear failure load
Optimization

ABSTRACT

Friction stir spot welding is a novel solid state process that has recently received considerable attention from various industries including automotive sectors due to many advantages over the resistance spot welding. However to apply this technique, the process parameters must be optimized to obtain improved mechanical properties compared to resistance spot welding. To achieve this, in this investigation, design of experiments was used to conduct the experiments for exploring the interdependence of the process parameters. A second order quadratic model for predicting the lap shear tensile strength of friction stir spot welded low carbon automotive steel joints was developed from the experimental obtained data. It is found that dwell time plays a major role in deciding the joint properties, which is followed by rotational speed and plunge depth. Further optimum process parameters were identified for maximum lap shear tensile strength using numerical and graphical optimization techniques.

1. Introduction

To meet the challenges in the today's automobile requirements, such as durability, reliability and sustainability, new emerging technologies were developed in the field of welding, since it plays a major role in many automobile components. In this manner, in order to weld low carbon automotive steel, commonly used technique in the automotive industry sector is the resistance spot welding (RSW). RSW has many limitations such as high wear rate of electrode, which limits the electrode life during welding of welding of steels [1], high temperature and rapid cooling rate leads to formation of brittle microstructure [2]. In order to avoid these limitations, friction stir spot welding (FSSW) process is the competent solid state process to weld the low carbon steel automotive steel. FSSW is a single spot joining process, in which a solid-state joining is made between adjacent materials at overlap configuration. This process also eradicates the problems associated with other conventional spot welding processes such as mechanical riveting, clinching, and toggle lock [3,4].

* *Corresponding author.*
E-mail: lakshminarayananak@ssn.edu.in (A.K. Lakshminarayanan).
http://dx.doi.org/10.1016/j.jmrt.2015.01.001

FSSW was initially limited to join aluminium alloy due to the difficulty in selecting the appropriate tool materials that can withstand the high temperature during friction stir spot welding of steels. However, with the development of new tool materials, now this process can be applied to weld steels. Aato et al. [5], used a probeless frictions stir spot welding tool to join low carbon steel plates. The rotating tool of 3.6 mm diameter, rotating at 18,000 rpm, was plunged into the upper plate at a rate of 0.2 mm/s, and then kept at a maximum plunged depth of 0.05–0.25 mm for 0–1 s (dwell time). In the weld obtained by this process, a hole due to the impression of the plunged tool probe was not formed.

Baek et al. [6], fabricated friction stir spot welded galvanized steel joints and reported that there was no mechanically mixed layer between the top and bottom plates at the weld nugget due to the limited tool penetration and the lower pin height of the welding tool than the steel plate thickness. Baek et al. [7], joined low carbon steel plates by friction stir spot welding (FSSW) with lap configuration and observed that the tool penetration depth exerted a strong effect on failure mode of joining samples and a weak effect on the joint shear strength. They also reported that, with increasing tool penetration depth, and consequently with increasing depth of the tool shoulder pressing into top sample, failure mode in a lap-shear test changed from brittle to ductile and concentrated near the pinhole located away from the weld towards base metal.

Sun et al. [8], investigated the microstructure and mechanical properties of mild steel joints prepared by a flat friction stir spot welding technique. The author observed that, during lap shear testing, when the weld failed through the interfacial mode, the load dropped to zero in a very short time after a failure. However, when the weld fracture through the plug failure mode, the applied load starts to drop as the crack initiates. Sun et al. [9] conducted a feasibility study on friction stir spot welding of low carbon steel plates with high frequency induction as an additional heat source and reported that with preheating, sound welds can be obtained with less amount of load and low rotational speed and also they observed that the shear tensile load also can reach a maximum value of 12.4 kN.

In FSSW, it is essential to understand the effect of process parameters such as rotational speed, dwell time and plunge depth on the weld quality characteristics [10–12]. In order to investigate the effect of these process parameters, most of the researchers follow the traditional experimental techniques by varying one parameter at a time while keeping the others constant. This conventional step-by step optimization approach involves a large number of independent runs and does not take into account the possible interactions between factors. To avoid these disadvantages, the use of design of experiment (DoE) is the most efficient means to reach conclusions with a minimum of trials. Though research work applying the design of experiments and response surface methodology on friction stir spot welding of aluminium alloys have been reported in literature [13–15], it appears that the empirical relationship between FSSW process parameters and quality characteristics (i.e. tensile shear failure load) of friction stir spot welded automotive steel has not been reported yet. Hence, in this investigation, design of experiments was used to conduct the experiments for exploring the interdependence of the process parameters and second order quadratic models for the prediction of tensile shear failure load of friction stir spot welded low carbon steel joints were developed from the data obtained by conducting the experiments.

Table 1 – Chemical composition of the base metal (measured).

Elements	C	Si	Mn	W	S	P	Fe
%	0.03	0.04	0.21	0.003	0.008	0.016	Remaining

2. Experimental work

2.1. *Identifying essential friction stir spot welding process parameters*

The base metal used in this investigation is low carbon automotive steels. The chemical composition and mechanical properties of the base metal are shown in Tables 1 and 2. From the feasibility study carried out in our laboratory, among many independently controllable primary and secondary process parameters affecting the tensile shear failure load, the process parameters of rotational speed (*N*), plunge depth (*P*), and dwell time (*D*), were selected for this study. These three are the parameters that decide the bonding characteristics and subsequently influencing the tensile shear failure load variations in the friction stir spot welded low carbon automotive sheets.

2.2. *Feasible limits of process parameters*

Trial runs were carried out using 0.8 mm-thick of low carbon automotive steel to find out the feasible working limits of FSSW process parameters. Different combinations of considered process parameters were used to carry out the trial runs. This was done by varying one of the factors from minimum to maximum, while keeping the rest of them at constant values. The feasible limits of the individual were identified by inspecting the flash formation, top surface of the weld, macrostructure (cross section of the weld) for a smooth appearance without any visible macro level defects such as pinhole and root defect. The chosen levels of the selected process parameters with their units and notations are presented in Table 3.

Table 2 – Mechanical properties of the base metal (Measured).

Property	Values
Ultimate tensile strength	365 MPa
Yield strength	305 MPa
Elongation	40%
Microhardness	105 $HV_{1.0}$

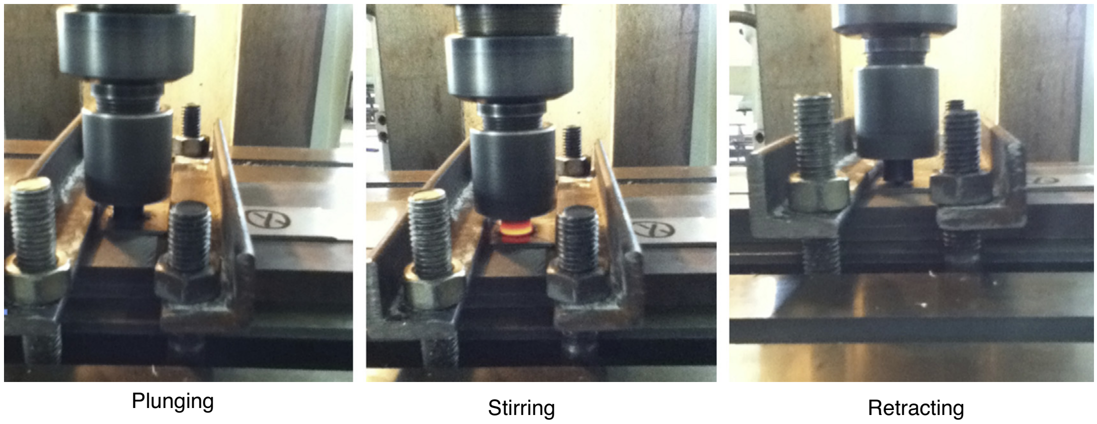

Fig. 1 – Different stages during FSSW of low carbon automotive steel.

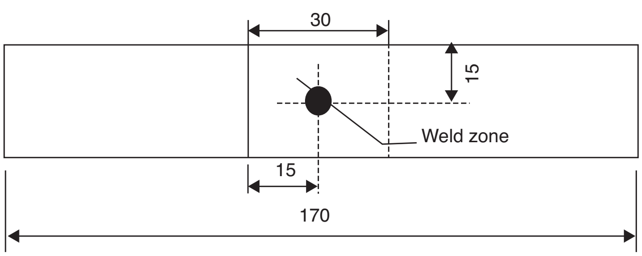

Fig. 2 – Dimension of lap shear tensile specimen.

2.3. *FSSW experiments and TSFL evaluation*

The friction stir spot welds were made as per the conditions dictated by the design matrix (Table 4) at random order so as to avoid the noise creeping output response. A non-consumable tool made up of tungsten based alloy was used to fabricate the joints. A tool with a flat cylindrical shoulder diameter of 8 mm is used and pin was tapered from 3.2 to 1.6 mm.

An indigenously developed friction stir welding machine was used to perform the FSSW process and the various stages of the process are shown in Fig. 1. At each condition, three specimens were fabricated. Lap shear tensile specimens are prepared as per the dimensions shown in Fig. 2. Some of the fabricated FSSW lap joints are displayed in Fig. 3. A lap shear tensile test was carried out in 100-kN electromechanically controlled Universal Testing Machine (FIE-Bluestar, India; model UNITEK-94100). The specimen was loaded at the rate of 1.5 kN/min as per ASTM specifications until the faying surfaces of the specimen were sheared off, and the values of tensile shear failure loads were recorded (Table 4).

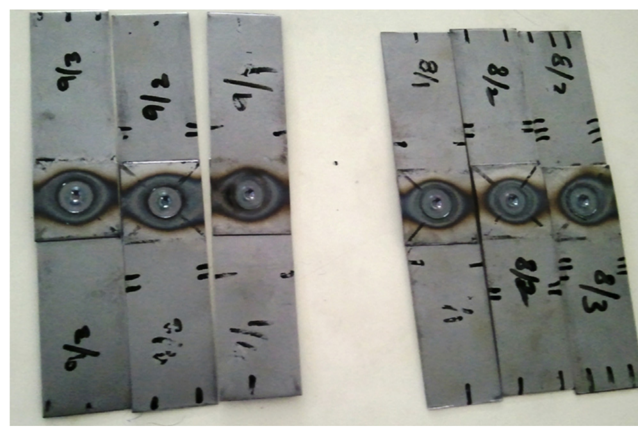

Fig. 3 – Some of fabricated friction stir spot welds.

3. Establishing an empirical relationship

In this investigation, the response surface methodology was used to predict maximum tensile shear failure load (TSFL) of automotive steel in terms of the friction stir spot welding process parameters. The application of response surface methodology to a welding procedure can be dealt elsewhere [16]. TSFL of friction stir spot-welded low carbon automotive steel is a function of the welding parameters such as tool rotational speed (*N*), plunge depth (*P*), and dwell time (*D*), and it can be expressed as,

$$\text{Tensile shear failure load (TSFL)} = f(N, P, D) \quad (1)$$

Table 3 – Feasible limits of the process parameters and their levels.

Parameters	Notation	Units	Levels				
			−1.682	−1	0	1	1.682
Rotational speed	N	rpm	1200	1281	1400	1519	1600
Plunge depth	P	mm	0	0.04	0.1	0.16	0.2
Dwell time	D	s	5	9	15	21	25

Table 4 – Design matrix and experimental results.

Exp. no	Coded value			Original value			TSFL (KN)
	N	*P*	*D*	*N*	*P*	*D*	
1	−1	−1	−1	1281	0.04	9	5.6
2	1	−1	−1	1519	0.04	9	9.5
3	−1	1	−1	1281	0.16	9	12.7
4	1	1	−1	1519	0.16	9	10.4
5	−1	−1	1	1281	0.04	21	10.3
6	1	−1	1	1519	0.04	21	15.5
7	−1	1	1	1281	0.16	21	12.1
8	1	1	1	1519	0.16	21	11.4
9	−1.682	0	0	1200	0.10	15	10.4
10	1.682	0	0	1600	0.10	15	12.8
11	0	−1.682	0	1400	0	15	9.9
12	0	1.682	0	1400	0.20	15	12.1
13	0	0	−1.682	1400	0.10	5	8.5
14	0	0	1.682	1400	0.10	25	13
15	0	0	0	1400	0.10	15	13.6
16	0	0	0	1400	0.10	15	13.4
17	0	0	0	1400	0.10	15	13.3
18	0	0	0	1400	0.10	15	13.5
19	0	0	0	1400	0.10	15	13.1
20	0	0	0	1400	0.10	15	13.4

The second-order polynomial (regression) equation used to represent the response surface Y is given by,

$$Y = b_o + \sum b_i x_i + \sum b_i {x_i}^2 + \sum b_{ij} x_i x_j + e_r \tag{2}$$

And for three factors, the selected polynomial could be expressed as,

Tensile shear failure load (TSFL)

$$= \{b_o + b_1(N) + b_2(P) + b_3(D) + b_{12}(NP) + b_{13}(ND) + b_{23}(PD) + b_{11}(N)^2 + b_{12}(P)^2 + b_{23}(D)^2\} \quad \text{in Newton} \tag{3}$$

The multiple linear regression coefficients for the second-order response surface model were calculated and the final empirical relationship was constructed using only these coefficients. The developed final empirical relationship is given below:

Tensile shear failure load (TSFL)

$$= \{13.38 + 0.74N + 0.69P + 1.37D - 1.51NP + 0.36ND - 1.29PD - 0.64N^2 - 0.85P^2 - 0.94D^2\} \quad \text{in kN} \tag{4}$$

The adequacy of the developed models were tested using the analysis of variance (ANOVA) technique and the results of second order response surface models fitted in the form of analysis of variance (ANOVA) are given in Table 5. The value of probability $P < F$ in Table 5 for model is less than 0.05, which indicates that the model is significant. In the same way, rotational speed (*N*), plunge depth (*P*) and dwell time (*D*), the interaction effect of rotational speed with plunge depth (*NP*), the interaction effect of plunge depth with dwell time (*PD*), interaction effect rotational speed with dwell time (*ND*) and second order term of rotational speed (*N*), plunge depth (*P*)

Table 5 – ANOVA for tensile shear failure load.

Source	Sum of squares	df	Mean square	*F* value	*p*-Value Prob > *F*	
Model	96.56494	9	10.72944	557.2028	<0.0001	Significant
N	7.523302	1	7.523302	390.7012	<0.0001	
P	6.469934	1	6.469934	335.9976	<0.0001	
D	25.51808	1	25.51808	1325.209	<0.0001	
NP	18.30125	1	18.30125	950.4233	<0.0001	
ND	1.05125	1	1.05125	54.59367	<0.0001	
PD	13.26125	1	13.26125	688.6852	<0.0001	
N^2	5.889903	1	5.889903	305.8754	<0.0001	
P^2	10.4472	1	10.4472	542.5454	<0.0001	
D^2	12.72887	1	12.72887	661.0375	<0.0001	
Residual	0.192559	10	0.019256			
Lack of fit	0.044226	5	0.008845	0.29815	0.8949	Not significant
Pure error	0.148333	5	0.029667			
Cor total	96.7575	19				

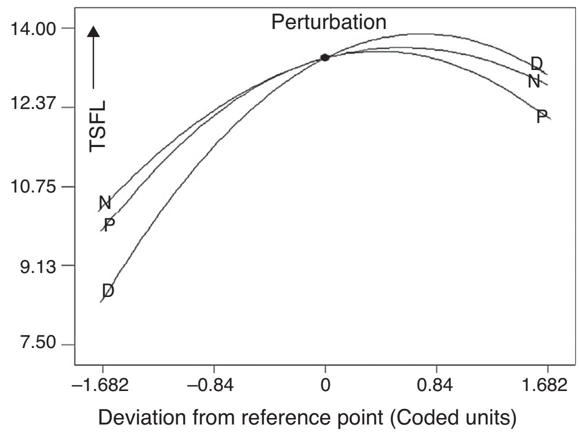

Fig. 4 – Perturbation plot showing effect of individual process parameters.

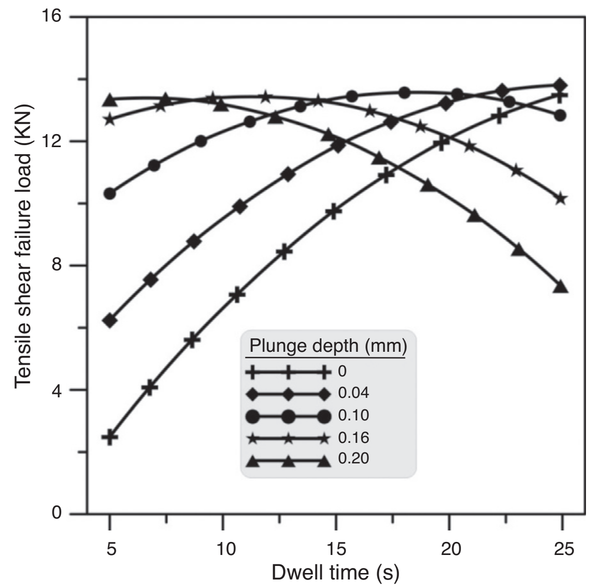

Fig. 5 – Interaction effect between dwell time and plunge depth.

and dwell time (*D*) has a significant effect on the tensile shear failure load. Lack of fit is non-significant, as it was desired. ANOVA indicates an excellent adequacy of the response surface model.

4. Effect of FSSW process parameters

In friction stir spot welding, the base metal is substantially modified due to the elevated temperature and intense plastic deformation during the process. The metallurgical bond at the joint interface and annular bond area decides the mechanical properties of friction stir spot welded steel joints. Table 6 shows the observations from fracture samples (top and bottom views of upper sheet and top view of lower sheet) of friction stir spot welded low carbon steel joints fabricated under different processing conditions. It is observed that, three different types of failure modes were observed after lap shear tensile testing due to the effect of different process parameters used. They are interfacial, simple nugget pullout and sheet tearing with extensive deformation. This can be very well correlated with the failure loads of frictions stir spot welded joints. The process parameter such as rotational speed, plunge depth and dwell time decides the joint properties of friction stir spot welds. The heat input and processing temperature during friction stir spot welding can be controlled by decreasing the rotational speed and dwell time. The consolidation between the top and bottom sheet during friction stir welding can be controlled by plunge depth of the tool. From the empirical relationship developed, the effect of process parameters on tensile shear failure load of friction stir spot welded low carbon automotive sheets is obtained and it is presented in the form of perturbation plot in Fig. 4. It is clear, that the TSFL increases with the increase of tool rotational speed, plunge depth, and dwell time to a certain value and then decreases. This is due to differences in the annular bond region formed and microstructural changes caused by the variations in process parameters, which also influence the failure mode of friction stir spot welded steel joints.

The maximum stir zone size increases with the rotational speed. In fact, an increase in the rotational speed results in more extensive stirring and formation of wider stir zone during FSSW. It has been reported that, the shear fracture of the nugget takes place easily, when the stir zone size is small, leading to lower tensile shear failure load [17]. With increasing rotational speed, the breaking load value was increased because of the higher heat generation that enlarged the stir zone size and so the bonded area [18]. However, too high rotational speed also lowers the mechanical properties due the high heat input, which results in grain growth in the stirred region. As per the ANOVA results, dwell time is the most influencing parameter on the tensile shear failure load of friction stir spot welded low carbon automotive steel. The

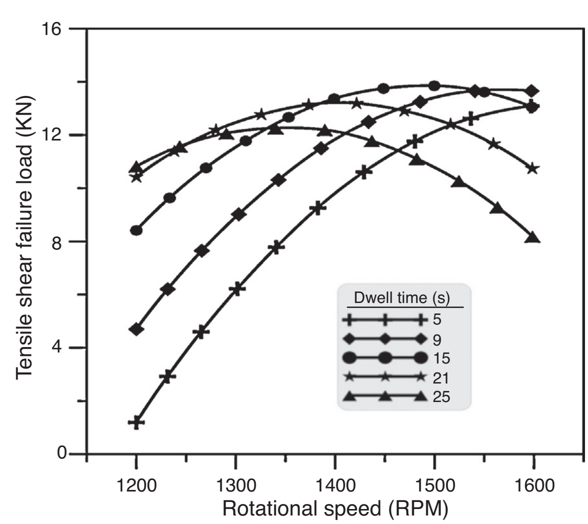

Fig. 6 – Interaction effect between rotational speed and dwell time.

Table 6 – Observations from fractured samples.

S. no.	Parameters	Top view of top sheet	Bottom view of top sheet	Top view of bottom sheet	Failure pattern
1.	N = 1281, P = 0.04, D = 9	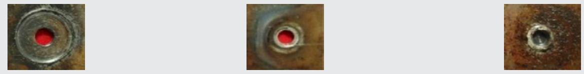			Interfacial
2.	N = 1519, P = 0.04, D = 9	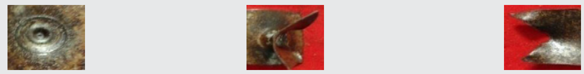			Nugget pullout
3.	N = 1281, P = 0.16, D = 9	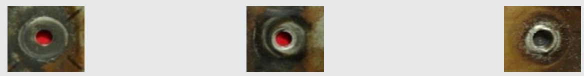			Partially curved interfacial
4.	N = 1519, P = 0.16, D = 9				Interfacial
5.	N = 1281, P = 0.04, D = 21	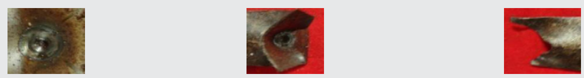			Nugget pullout
6.	N = 1519, P = 0.04, D = 21	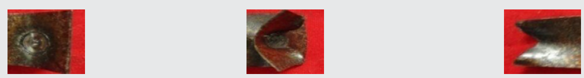			Nugget pullout
7.	N = 1281, P = 0.16, D = 21	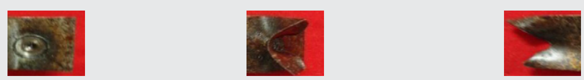			Nugget pullout
8.	N = 1519, P = 0.16, D = 21				Interfacial
9.	N = 1200, P = 0.10, D = 15	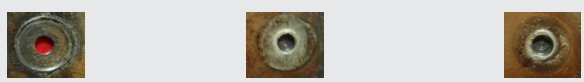			Nugget pullout
10.	N = 1600, P = 0.10, D = 15	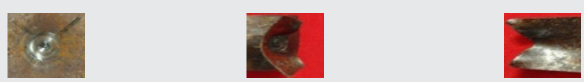			Nugget pullout
11.	N = 1400, P = 0.00, D = 15	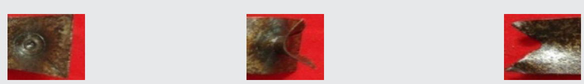			Nugget pullout
12.	N = 1400, P = 0.20, D = 15	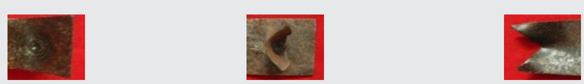			Nugget pullout
13.	N = 1400, P = 0.10, D = 5	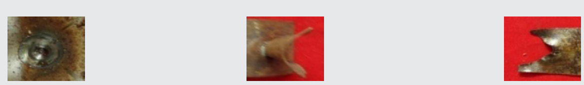			Nugget pullout
14.	N = 1400, P = 0.10, D = 25	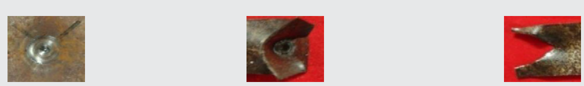			Nugget pullout
15.	N = 1400, P = 0.10, D = 15	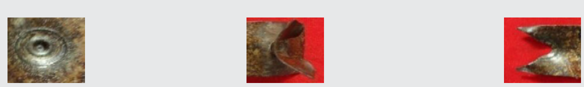			Nugget pullout

effect annular bond region during stirring is increased with the increase in dwell time and thereby improving the mechanical properties of the spot welds. Similarly, increasing in plunge depth improves the consolidation of the weld by effective diffusion of atoms between the top and bottom plates. However, higher plunge depth resulted in weaker joint due to the thinning of the top sheet.

Though the effect of individual process parameter follows a trend as shown in Fig. 4, there is a strong interaction effect of the process parameters on the tensile shear failure load, which is evidenced from Figs. 5 and 6. To understand the effect of process parameters, the macrostructure and corresponding load displacement curves of three joints, which yielded low, medium and high tensile shear failure loads are presented in Figs. 7 and 8. From the macrostructure presented in Fig. 7, it is inferred that the material from the bottom sheet was extruded and pushed upward closer to the pinhole irrespective processing condition used. This caused the joint interface to become a curved line indicating that the material was subjected severe plastic deformation during friction stirring. However, an unmixed region is observed in Fig. 7a and this indicates that the joint bonding was initiated, but not completed in full due to an unoptimized processing condition. Fig. 7b displays a defect free macrostructure with increased

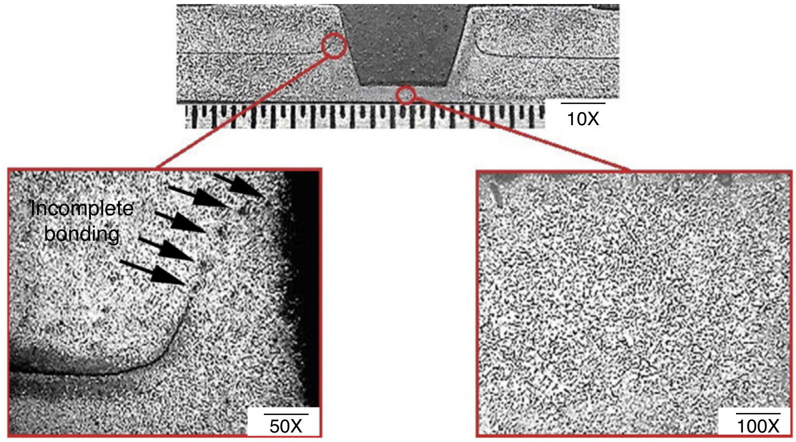

a Representative macrostructure yield lower tensile failure load

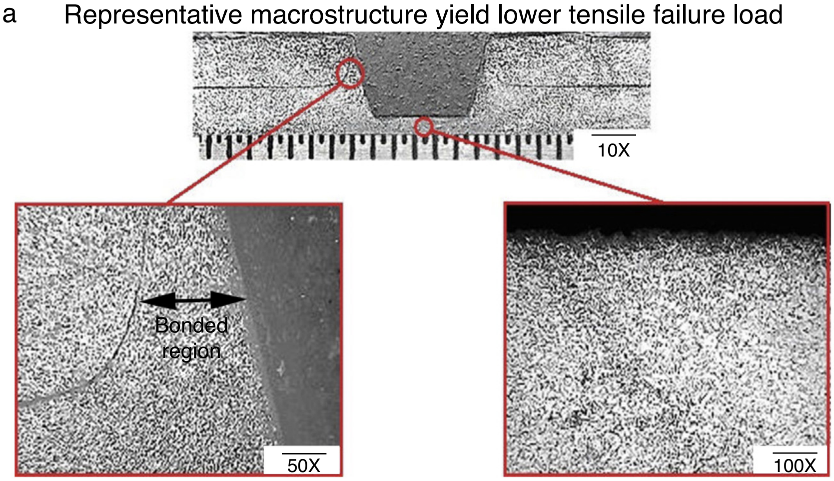

b Representative macrostructure yielded highest tensile failure load

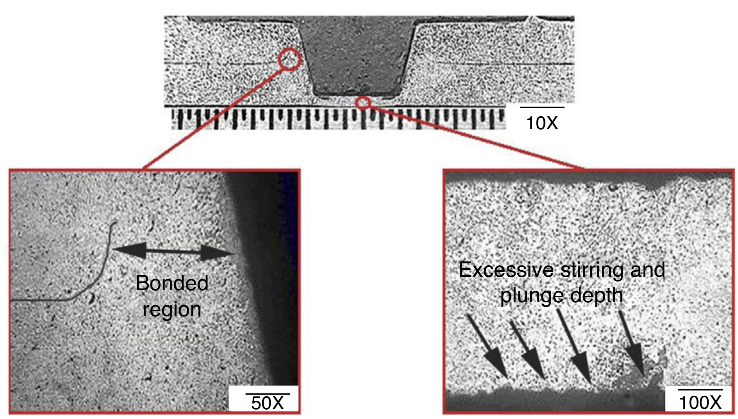

c Representative macrostructure yielded medium tensile failure load

Fig. 7 – Macrostructure of friction stir spot welded low carbon automotive steel.

bond length due to the application of optimized process parameters. Though the bond length is higher in the case of the macrostructure shown in Fig. 7c, the joints showed inferior tensile shear failure loads compared to its counterpart due to the extrusion of more metal towards the shoulder region and poor surface roughness caused by an excess forging action.

From the tensile shear failure load deformation curves presented in Fig. 8, it is observed that during lap shear tensile testing, the crack was initiated from unmixed region and reached the pinhole by propagating the stir zone. The joints failed in interfacial mode yielded lower tensile shear failure as it is expected. The joints, which recorded medium and highest failure loads showed nugget pullout by sheet tearing. However, the crack was initiated in the bottom sheet for the joint, which yielded medium failure load due excessive forging condition exerted by the processing conditions used. Whereas, the failure was initiated in the top sheet for the joint, which yielded maximum tensile shear failure load with extensive

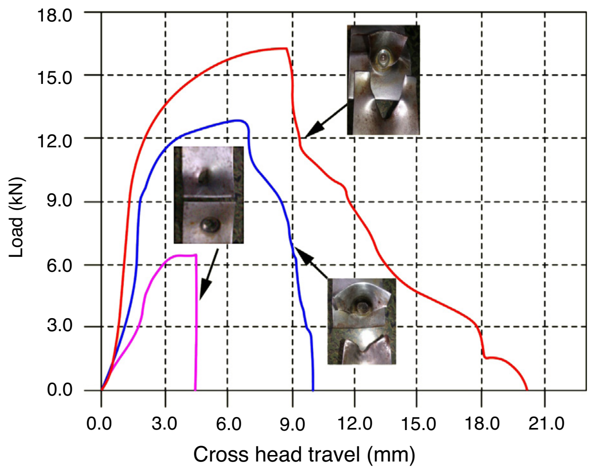

Fig. 8 – Load–displacement curves of low carbon automotive FSSW steel joints.

deformation due to proper metallurgical bonding and refined grain size of stir zone.

The microstructure of friction stir spot welded low carbon steel joint that yielded highest strength was analyzed and is displayed in Fig. 9. Six different regions, namely stirzone, thermomechanical affected zone, heat affected zone, partially bonded region and unbonded region were observed in friction stir spot welded low carbon automotive steel. The annealed ferritic phase of the base metal with the average grain size of 25 μm is changed into fine equiaxed ferrite with average grain size of 6 μm in stir zone, 8 μm in TMAZ and 30 μm in HAZ. EDS elemental mapping indicated that some oxides are formed and entrapped at the interface of partially bonded region. These oxides may be formed by surface oxidation during the plunge stage of welding and later incorporated into the interface along the partially bonded region. However, the effect these oxides on the tensile shear failure load and failure mode is not known and need to be evaluated by further research.

5. Finding optimum process parameters

The response surface methodology (RSM) was used to optimize the parameters in this study. To obtain the influencing nature and optimized condition of the process on TSFL, the contour plots, which indicate the possible independence of factors, have been developed for the proposed empirical relation by considering one parameter in the middle level and two parameters in the *x*- and *y*-axes as shown in Fig. 10. These contours can help in the prediction of the response (TSFL) for any zone of the experimental domain. A contour plot is also produced to display the region of the optimal factor settings visually. By analyzing the contour plots (Fig. 10a–c), stationary point can be obtained around which, the optimized values are available. In this investigation, numerical optimization was carried out using Design Expert Software V.8.0. The numerical optimization feature in the design expert package uses downhill pattern search algorithm and finds one point or more in the factors domain that would maximize the objective function [19]. The optimization module in design-expert searches for a combination of factor levels that simultaneously satisfy the requirements placed (i.e. optimization criteria) on the response and process factors. Based on the numerically solved values, overlay plot is constructed and the maximum tensile shear failure load (optimum) is located in Fig. 10d.

6. Validation experiments using optimized values

FSSW experiments were conducted to verify the accuracy of the developed empirical relationship presented in Eq. (4). Three friction stir spot welds were made using different values of rotational speed, plunge depth and dwell time randomly chosen from the optimized values based on desirability values other than that what were used in the design matrix. The results obtained were quite satisfactory and the details are presented in Table 7.

Table 7 – Confirmation experiments.

Exp. no.	*N* (rpm)	*P* (mm)	*D* (s)		Tensile shear failure load (KN)
1	1530	0.05	21.3	Actual	14.97
	(1.09)	(−0.97)	(1.07)	Predicted	15.72
				Error %	4.96
2	1595	0.05	22.8	Actual	15.50
	(1.64)	(−0.95)	(1.32)	Predicted	16.38
				Error %	5.37
3	1591	0.05	19.64	Actual	15.73
	(1.61)	(−0.96)	(0.78)	Predicted	14.98
				Error %	4.77

Values given in the brackets are the corresponding coded values.

$$\%\text{Error} = \frac{\text{Measured value} - \text{predicted value}}{\text{Predicted value}}$$

J MATER RES TECHNOL. 2015;4(3):262–272

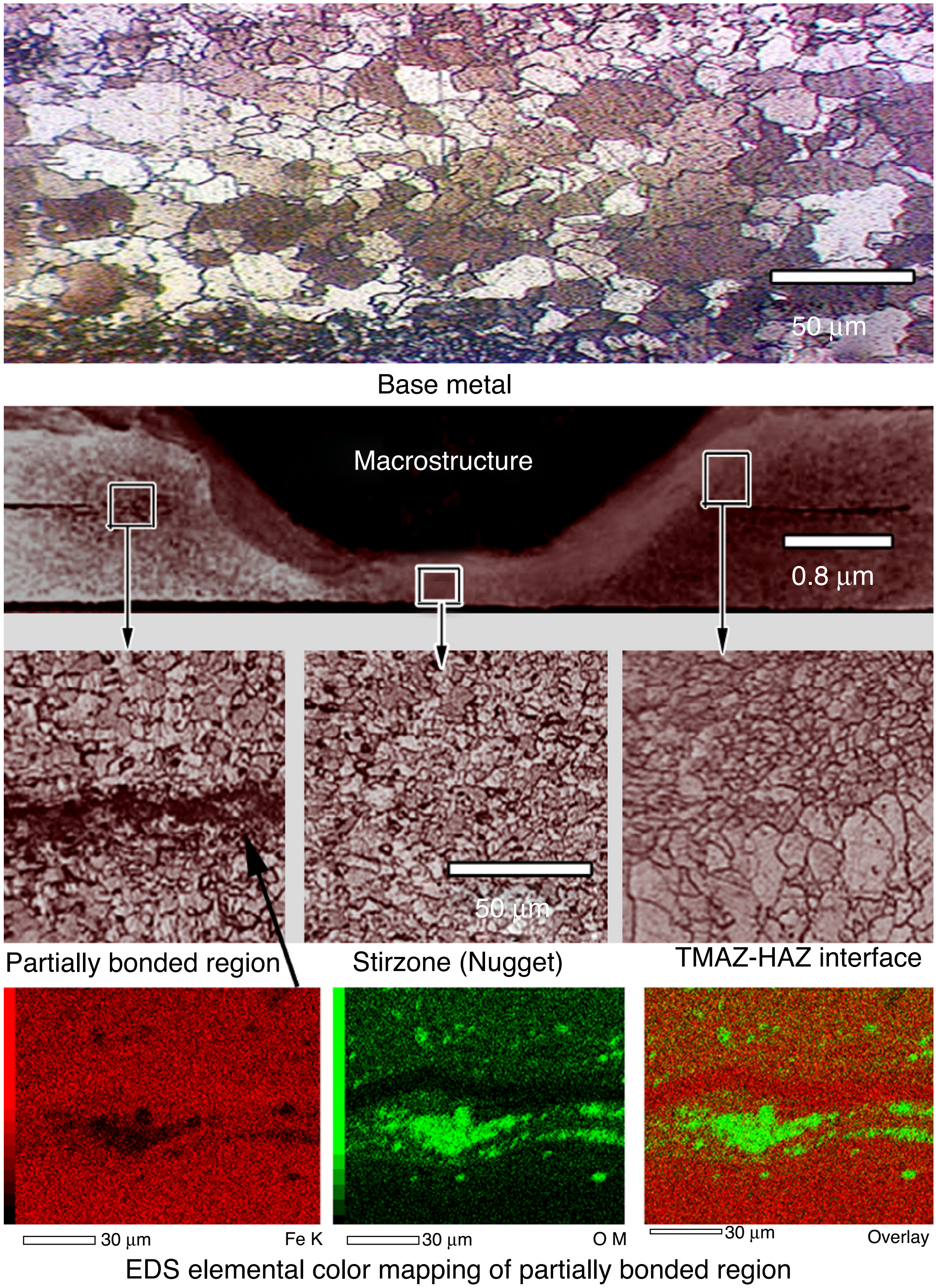

Fig. 9 – Microstructural analysis of low carbon automotive FSSW steel joints.

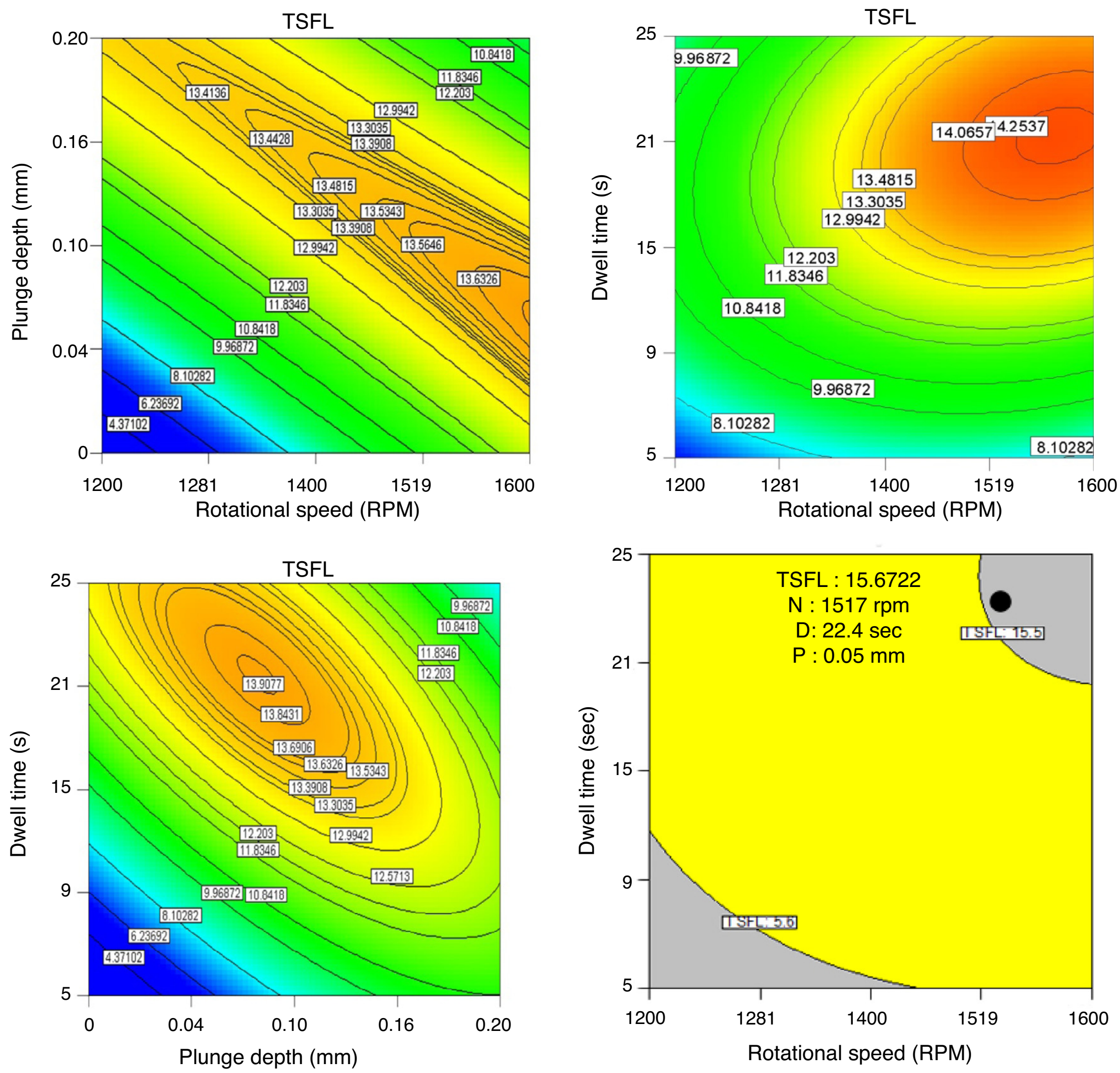

Fig. 10 – Contour graphs and graphical optimization.

7. Conclusions

Empirical relationship developed from the experimental data obtained during friction stir spot welding of low carbon automotive steel was employed to study the relationship between tensile shear failure load and process parameters.

- Of the four parameters investigated, dwell time is found to have great influence on tensile shear fracture load (TSFL) followed by tool rotation speed and plunge depth.
- Interaction effect between the rotational speed and plunge depth, plunge depth and dwell is also having the predominant influence on tensile shear failure load and failure modes.
- A maximum tensile shear fracture load of 15.67 kN could be attained under the welding conditions of 1157 rpm of tool rotation speed, 0.05 mm of plunge depth and 22 s of dwell time. In this case, the maximum elongation was observed where the joint failure in sheet tearing mode.

Conflicts of interest

The authors declare no conflicts of interest.

Acknowledgement

The authors are grateful to Department of Science and Technology, Government of India for their financial support through a funded research project No: SR/S3/ME041/2007.

REFERENCES

[1] Sun HT, Lai XM, Zhang YS, Shen J. Effect of variable electrode force on weld quality in resistance spot welding. Sci Technol Weld Join 2007;12:718–24.

[2] Choi HS, Park G, Lim W, Kim B. Evaluation of weldability for resistance spot welded single-lap joint between GA780DP and hot-stamped 22MnB5 steel sheets. J Mech Sci Technol 2011;25:1543–50.

[3] Malafaia AMS, Milan MT, Oliveira MF, Spinelli D. Fatigue behavior of friction stir spot welding and riveted joints in an Al alloy. Procedia Eng 2010;2:1815–21.
[4] Briskham P, Blundell N, Han L, Hewitt R, Young K, Boomer D. Comparison of self-pierce riveting, resistance spot welding and spot friction joining for aluminium automotive sheet, SAE Int Tech pap 2006, Paper No: 2006-01-0774.
[5] Aota K, Ikeuchi K. Development of friction stir spot welding using rotating tool without probe and its application to low-carbon steel plates. Weld Int 2009;23:572–80.
[6] Baek SW, Choi DH, Lee CY, Ahn BW, Yeon YM, Song K, et al. Microstructure and mechanical properties of friction stir spot welded galvanized steel. Mater Trans 2010;51: 1044–50.
[7] Baek SW, Choi DH, Lee CY, Ahn BW, Yeon YM, Song K, et al. Structure–properties relations in friction stir spot welded low carbon steel sheets for light weight automobile body. Mater Trans 2010;51:399–403.
[8] Sun YF, Fujii H, Takaki N, Okitsu Y. Microstructure and mechanical properties of mild steel joints prepared by a flat friction stir spot welding technique. Mater Des 2012;37:384–92.
[9] Sun YF, Shen JM, Morisada Y, Fujii H. Spot friction stir welding of low carbon steel plates preheated by high frequency induction. Mater Des 2014;54:450–7.
[10] Klobcar D, Tusek J, Skumavc A, Smolej A. Parametric study of friction stir spot welding of aluminium alloy 5754. Metalurgija 2014;53:21–4.
[11] Tutar M, Aydin H, Yuce C, Yavuz N, Bayram A. The optimisation of process parameters for friction stir spot-welded AA3003-H12 aluminium alloy using a Taguchi orthogonal array. Mater Des 2014;63:789–97.
[12] Al-Shahrani A, Wynne BP. Effect of dwell time on friction stir spot welded dual phase steel. Adv Mater Res 2009;83–86:1143–50.
[13] Muhammad N, Yupiter Manurung HP, Hafidzi M, Abas SK, Tham G, Haruman E. Optimization and modeling of spot welding parameters with simultaneous multiple response consideration using multi-objective Taguchi method and RSM. J Mech Sci Technol 2012;26:2365–70.
[14] Pieta G, Santos JD, Strohaecker TR, Clarke T. Optimization of friction spot welding process parameters for AA2198-T8 sheets. Mater Manuf Processes 2014;29:934–40.
[15] Kim T, Park H, Rhee S. Optimization of welding parameters for resistance spot welding of TRIP steel with response surface methodology. Int J Prod Res 2005;43:4643–57.
[16] Benyounis KY, Olabi AG. Optimization of different welding processes using statistical and numerical approaches – a reference guide. Adv Eng Softw 2008;39:483–96.
[17] Tozaki Y, Uematsu Y, Tokaji K. A newly developed tool without probe for friction stir spot welding and its performance. J Mater Process Technol 2010;210:844–51.
[18] Hong SH, Sripichai K, Yu CS, Avery K, Pan J, Pan TY, et al. Failure modes of friction stir spot welds in lap-shear specimens of dissimilar advanced high strength steels under quasi-static and cyclic loading conditions. SAE Int J Mater Manuf 2012;5:375–81.
[19] Lakshminarayanan AK, Balasubramanian V. Understanding the parameters controlling friction stir welding of AISI 409M ferritic stainless steel. Met Mater Int 2011;17:969–81.